Involvement of the CP47 Protein in Stabilization and Photoactivation of a Functional Water-Oxidizing Complex in the Cyanobacterium *Synechocystis* sp. PCC 6803†

Hermann M. Gleiter,[‡,||] Elisabeth Haag,[‡,⊥] Jian-Ren Shen,[§] Julian J. Eaton-Rye,[#,▽] Angela G. Seeliger,[‡] Yorinao Inoue,[§] Wim F. J. Vermaas,[#] and Gernot Renger*[,‡]

Max-Volmer-Institute for Physical and Biophysical Chemistry, Technical University Berlin, D10623 Berlin, Germany, Solar Energy Research Group, The Institute of Physical and Chemical Research (RIKEN), Wako, Saitama, 351-01 Japan, and Department of Botany, Arizona State University, Tempe, Arizona 85287-1601

Received December 19, 1994; Revised Manuscript Received February 28, 1995[⊗]

ABSTRACT: Oscillation patterns of the oxygen yield per flash induced by a train of single-turnover flashes were measured as a function of dark incubation and different pre-illumination conditions in several autotrophic mutant strains of *Synechocystis* sp. PCC 6803 carrying short deletions within the large, lumen-exposed hydrophilic region (loop E) of the chlorophyll *a*-binding photosystem II protein CP47. A physiological and biochemical characterization of these mutant strains has been presented previously [Eaton-Rye, J. J., & Vermaas, W. F. J. (1991) *Plant Mol. Biol. 17*, 1165−1177; Haag, E., Eaton-Rye, J. J., Renger, G., & Vermaas, W. F. J. (1993) *Biochemistry 32*, 4444−4454], and some functional properties were described recently [Gleiter, H. M., Haag, E., Shen, J.-R., Eaton-Rye, J. J., Inoue, Y., Vermaas, W. F. J., & Renger, G. (1994) *Biochemistry 33*, 12063−12071]. The present study shows that in several mutants the water-oxidizing complex (WOC) became inactivated during prolonged dark incubation, whereas the WOC of the wild-type strain remained active. The rate and extent of the inactivation in the mutants depend on the domain of loop E, where 3−8 amino acid residues were deleted. The most pronounced effects are observed in mutants Δ(A373−D380) and Δ(R384−V392). A competent WOC can be restored from the fully inactivated state by illumination with short saturating flashes. The number of flashes required for this process strongly depends on the site at which a deletion has been introduced into loop E. Again, the most prominent effects were found in mutants Δ(A373−D380) and Δ(R384−V392). Interestingly, the number of flashes required for activation was reduced by more than an order of magnitude in both mutants by the addition of 10 mM $CaCl_2$ to the cell suspension. On the basis of a model for photoactivation proposed by Tamura and Cheniae (1987) [*Biochim. Biophys. Acta 890*, 179−194], a scheme is presented for the processes of dark inactivation and photoactivation in these mutants. The results presented here corroborate an important role of the large hydrophilic domain (loop E) of CP47 in a functional and stable WOC.

The fundamental process of photosynthetic water cleavage is the oxidation of two H_2O molecules to dioxygen and four protons. In all oxygen-evolving photoautotrophic organisms, this reaction takes place within a multimeric pigment-protein complex referred to as photosystem II (PSII)[1] which is anisotropically incorporated into the thylakoid membrane [for reviews, see Babcock (1987), Renger (1987a), Ikeuchi (1992), and Vermaas et al. (1993)]. Two indispensable prerequisites are required to perform water oxidation: (a) the generation of sufficiently oxidizing redox equivalents (holes) and (b) the cooperation of four holes. The former goal is achieved by light-induced electron ejection from the lowest excited singlet state of a special chlorophyll *a* species (designated as P680), with pheophytin (Pheo) as the primary acceptor, and subsequent rapid electron transfer from $Pheo^-$ to a special plastoquinone, Q_A [for a recent review, see Renger (1992)]. The latter reaction comprises a sequence of univalent electron abstraction steps from a manganese-containing unit referred to as the water-oxidizing complex (WOC).

Although significant progress has been achieved in understanding the process of photosynthetic water oxidation, especially with respect to the kinetic pattern [for recent reviews, see Rutherford et al. (1992), Debus (1992), and Renger (1993)], key mechanistic questions still remain to be answered [for a list, see Renger (1987b, 1993)]. Also, the structure of the water oxidase and the nature of its protein matrix are not yet resolved. Regarding the latter problem, current research activities focus on two questions: (i) What is the structure of the manganese cluster and its coordination sphere? (ii) Which polypeptides provide ligands to the manganese? Recent EXAFS studies have provided informa-

† Financial support by the Deutsche Forschungsgemeinschaft (Re 354/11-3) is gratefully acknowledged. W.V. was supported by U.S. Department of Energy Grant DE-FG02-89 ER 14031.

* Corresponding author (fax 49-30-31421122).
‡ Technical University Berlin.
§ RIKEN.
|| Present address: Institute of Physiology, Philipps, University Marburg.
⊥ Present address: Institute of Biology, Humboldt University, Berlin.
Arizona State University.
▽ Present address: Department of Biochemistry, Otago University, Dunedin, New Zealand.

⊗ Abstract published in *Advance ACS Abstracts,* April 15, 1995.

[1] Abbreviations: Chl, chlorophyll; HEPES, 4-(2-hydroxyethyl)-1-piperazineethanesulfonic acid; PSII, photosystem II; PSII-O, extrinsic regulatory protein encoded by the *psbO* gene; WOC, water-oxidizing complex; WT, wild type; Pheo, pheophytin.

0006-2960/95/0434-6847$09.00/0

tion on the nuclear geometry of the manganese. It was shown that the experimental findings can be best explained by dimer models of two binuclear manganese clusters (Kusunoki et al., 1993; Klein et al., 1993; Yachandra et al., 1993). It seems very likely that the tetranuclear manganese complex exhibits functional heterogeneity with one dimer directly participating in the redox reactions that lead to the intermediary storage of holes and the eventual formation of dioxygen [Mukerji et al., 1994; for further discussion, see Renger (1993)].

Within the framework of the five-state conventional Kok model (Kok et al., 1970), the WOC is assumed to undergo a cyclic pathway of univalent oxidation steps from states S_0 to S_4, returning to S_0 after O_2 release. Exogenous reductants like NH_2NH_2 and NH_2OH can interact with the WOC in such a way that the superreduced redox states S_{-1} and S_{-2} are formed [for a recent study, see Messinger and Renger (1993) and references therein]. A more extensive treatment with these substances leads to reductive loss of the manganese and complete elimination of the oxygen evolution capacity (Cheniae & Martin, 1970). However, this activity can be restored in the presence of exogenous Mn^{2+} and suitable electron acceptors by a process called photoactivation (Radmer & Cheniae, 1977). A sequence of two light-driven reactions separated by a dark process gives rise to proper incorporation and ligation of manganese (Klimov et al., 1990; Miyao & Inoue, 1991; Tamura et al., 1991; Blubaugh & Cheniae, 1992). Recently, synthetic binuclear manganese-(III) complexes were shown to be especially efficient in restoring the WOC by photoactivation (Allakhverdiev et al., 1994). A maximum level of activity was achieved at a stoichiometry of four manganese in the assay and in the presence of the extrinsic 33 kDa protein [designated as PSII-O protein; see Vermaas et al. (1993)]. The latter effect indicates that the PSII-O protein plays an essential role in stabilizing the WOC.

Different lines of experimental evidence suggest that the PSII-O protein binds to the intrinsic chlorophyll *a*-binding protein CP47, which is an integral part of the PSII core complex: (i) extraction of PSII-O protein increases the susceptibility to proteolytic enzymes, labeling reagents, and/or antibodies against CP47 (Bricker & Frankel, 1987; Bricker et al., 1988; Frankel & Bricker, 1990); (ii) cross-linking experiments suggest close proximity between the PSII-O protein and CP47 (Enami et al., 1987, 1989, 1991; Bricker et al., 1988; Odom & Bricker, 1992); and (iii) on the basis of experiments of limited proteolysis, the domain around K389 of CP47 is inferred to be important in binding the PSII-O protein and maintaining high oxygen evolution (Hayashi et al., 1993). This region is located in the C-terminal part of the putative large hydrophilic loop between transmembrane helices V and VI, which is assumed to be exposed to the lumenal side (Vermaas et al., 1987; Bricker, 1990). All data available so far are in line with the idea that the N-terminus of PSII-O interacts with a domain between residues 364 and 440 of CP47 (Eaton-Rye & Murata, 1989; Frankel & Bricker, 1990; Odom & Bricker, 1992). Accordingly, CP47 and, in particular, this domain of the extended loop (designated as loop E) appear to be relevant structural elements in establishing a functionally competent WOC. This question has been addressed by introducing targeted mutations and deletions into the *psbB* gene, which encodes CP47. It was shown that specific parts of loop E are important not only for the WOC but also for the assembly of a stable PSII core complex (Haag et al., 1993). A previous study revealed that deletion of charged and conserved amino acid residues (deletion length: 3−8 residues) from the region roughly located between residues 370 and 390 decreases the binding of PSII-O without imposing a high demand for Ca^{2+} for photoautotrophic growth. The most striking feature, however, is the modification of the characteristic period four oscillation of flash-induced oxygen formation after long dark adaptation and its complete reappearance in the "normal" shape after light activation (Gleiter et al., 1994). These results were interpreted to possibly reflect mutation-induced alterations of dark inactivation/light activation processes of the WOC (Haag, 1993; Gleiter et al., 1994).

In the present study, the deactivation/photoactivation processes were studied in detail by measurements of thermoluminescence and flash-induced oxygen evolution. It is shown that particular deletions from loop E of CP47 give rise to significantly reduced dark stability of a fully functional WOC. Likewise, the number of flashes required for restoration of the characteristic period four oscillation pattern are much larger in these mutants than in the wild type and are shown to be influenced very significantly by the presence of Ca^{2+}. The implications of these findings will be discussed.

MATERIALS AND METHODS

Mutant Construction. Targeted mutagenesis of the *psbB* gene, leading to CP47 deletion mutants in the cyanobacterium *Synechocystis* sp. PCC 6803, and verification of the mutation have been described previously (Eaton-Rye & Vermaas, 1991; Haag et al., 1993). The control strain (Eaton-Rye & Vermaas, 1991) is genetically identical to the mutant strains except for the mutation in *psbB*.

Cell Culture and Growth. Liquid cultures of control and mutant strains were cultivated at 30 °C in regular BG-11 medium (Rippka et al., 1979) supplemented with 5 mM glucose and 20 μg/mL kanamycin. During propagation on solid agar plates (BG-11 medium containing 1.5% (w/v) agar, 0.3% $Na_2S_2O_3$, and 10 mM TES/NaOH, pH 8.2), atrazine (20 μM) was also added to the medium in order to inhibit PSII activity and, thus, to reduce selective pressure for (pseudo)revertants. The light intensity of the growth chamber was 60 $\mu E/m^2 s$.

Deactivation and Activation of the Water-Oxidizing Complex. Cells were washed with buffer solution (10 mM NaCl and 25 mM Hepes/NaOH, pH 7.0) and then illuminated for 5 min with white light. After a definite time of dark incubation at room temperature, the oscillation patterns were measured. For activation experiments the cells were treated in the same way, but the dark incubation at room temperature was 48 h. These cells were put onto the Joliot-type electrode and illuminated with a certain number of flashes at a frequency of 1 Hz. After an additional 3 min dark adaptation at room temperature following the activation period of flash illumination, the oscillation patterns of flash-induced oxygen yield were measured. For activation experiments with $20 \leq N \leq 480$ flashes, the following procedure was used: dark-adapted cells on the Joliot-type electrode were illuminated with groups of 20 flashes at a frequency of 1 Hz and a time of 3 min between flash groups. The polarization of the electrode was switched off during the dark time and turned

on 30 s before each flash train. The polarographic signals induced by each train of 20 flashes were monitored (vide infra). When the number of activation flashes exceeded 480, the procedure was continued, but the frequency of activating preflashes was increased to 9 Hz. Control experiments were performed with samples illuminated outside the Joliot-electrode with $480 \leq N \leq 12\,000$ flashes at 9 Hz. After 3 min dark adaptation the oscillation pattern was measured. No significant differences were observed. This indicates that incubation of the cells on the Joliot electrode does not cause significant changes in the activity.

Flash-Induced Thermoluminescence. Thermoluminescence was measured with the setup described in Rutherford et al. (1982, 1984). Cells were pre-illuminated with 500 saturating flashes, followed by dark incubation of different lengths (as indicated in the figure legends). For charge separation, the samples (concentration: 100 μM chlorophyll) were excited at room temperature with a saturating flash from a xenon lamp (FWHM $\approx$ 10 μs) and rapidly cooled down to 77 K. The heating rate for eliciting thermoluminescence emission was 1 K/s.

Flash-Induced Oxygen Evolution. The pattern of the oxygen yield per flash induced by a train of short saturating flashes from a xenon lamp (FWHM $\approx$ 3 μs) was monitored at 20 °C with a Joliot-type electrode (Joliot, 1972), which keeps the temperature constant within ±0.2 °C. The polarization voltage of −750 mV was switched on 30 s before the measurements. Further experimental details are given in Messinger and Renger (1990) and Gleiter et al. (1994).

The normalized population of the S_i states was calculated within the framework of an extended Kok model, comprising the superreduced states S_{-1} and S_{-2} as outlined in Messinger et al. (1991). The signal of the first flash was omitted for mutants, because it is very likely due to processes other than oxygen formation via the normal Kok cycle (vide infra).

RESULTS

The physiological and biochemical properties of the CP47 mutants analyzed in this study have been described in preceding publications (Eaton-Rye & Vermaas, 1991; Haag et al., 1993). A more detailed characterization of the binding properties of the PSII-O protein and some functional properties are presented in Gleiter et al. (1994). In the present communication, only those mutants that exhibit significant oxygen evolution capacity were investigated (≥50% of the WT control). They include the mutant strains Δ(G333−I336), Δ(K347−R352), Δ(A373−D380), Δ(R384−V392), Δ(V392−Q394), and Δ(D416−F420), where Δ indicates a short deletion from loop E of the CP47 polypeptide, and the deleted amino acid residues are given in parentheses.

Modification of the Water-Oxidizing Complex by Dark Incubation. Figure 1 shows typical traces of the polarographic signals measured in *Synechocystis sp.* PCC 6803 cells of wild type (WT) and mutant Δ(A373−D380), excited with a train of 20 flashes (1 Hz) that followed two different times of dark incubation after 5 min of pre-illumination. Two interesting features emerge from these results: (a) At comparatively short dark incubation times of less than 30 min both samples [WT and mutant Δ(A373−D380)] exhibit a characteristic period four oscillation pattern. (b) After 24 h of dark incubation the oscillation of the Δ(A373−D380) mutant disappeared completely, accompanied by a marked decrease in the amplitude and change in shape of the signals; however, in WT cells, the period four pattern is only slightly modified (an oscillation pattern—although in a highly damped form—is still discernible even after a much longer dark incubation of 72 h; data not shown). A closer inspection of the data reveals that, in contrast to thylakoids from spinach [for a recent study, see Messinger and Renger (1994)], a significant signal arises following the first flash. The shape of this signal and also that of the signal caused by the second flash differ from that caused by the subsequent flashes. The "first-flash phenomenon" is a well-known phenomenon in several cyanobacteria like *Oscillatoria chalybea* (Bader et al., 1983). Mass spectroscopic studies revealed that it reflects—at least in part—flash-induced oxygen evolution (Bader et al., 1994), but the dependence of this signal on different parameters [e.g., dark incubation time; see Bader (1994)] indicates that this oxygen presumably originates from H_2O_2. A similar feature of a first-flash polarographic signal has been observed in PSII membrane fragments from spinach and was also interpreted to originate from H_2O_2 (Seibert & Lavorel, 1983). On the other hand, recent studies show that flash-induced polarographic signals can also arise in *Synechocystis sp.* PCC 6803 mutants lacking PSII (Gleiter et al., 1994). Therefore, the origin of this signal is not fully resolved. However, it must be emphasized that the first (and second) signal is not relevant for the conclusions gathered from the data of the present study. Regardless of this special effect of the first (and second) flash, the data of Figure 1 suggest that the functional state of the WOC markedly changes in the dark. The most striking feature of WT cells is a shift in the maximum oxygen yield from the third to the fourth flash, which is reminiscent of a shift in the dark redox state of either the WOC from S_1 to S_0 or, alternatively, Y_D^{ox} to Y_D (Messinger & Renger, 1994). A much more dramatic effect is observed in the cells of mutant strain Δ-(A373−D380). In this case, not only is the oscillation pattern entirely suppressed but, more importantly, the functional activity of the WOC becomes highly impaired. A qualitatively similar but less pronounced effect has been observed in a previous study (Gleiter et al., 1994). This observation was interpreted as an inactivation of the WOC due to a modified structure of CP47 that gives rise to markedly weaker binding of the PSII-O protein (Haag, 1993; Gleiter et al., 1994).

In order to analyze, by an independent method, the dark relaxation of the WOC in the mutants compared to the WT, thermoluminescence measurements were performed. This technique is a very useful tool to analyze the redox properties of the donor and acceptor sides of PSII [for a recent review, see Vass and Inoue (1992)]. The characteristic B-band in particular, which is observed if samples are transferred to the redox state $S_2Q_B^-$ by excitation with a single-turnover flash in the absence of DCMU, provides information on the population and redox properties of the couples S_2/S_1 and Q_B^-/Q_B. Accordingly, under conditions of approximately identical PSII concentrations in the different samples, the peak height of the B-band reflects the population probability of the redox state S_1Q_B before flash excitation. As the PSII content varied among different mutants [see Haag et al. (1993)], the signals measured after various dark incubation times were normalized to the amplitude of the B-band

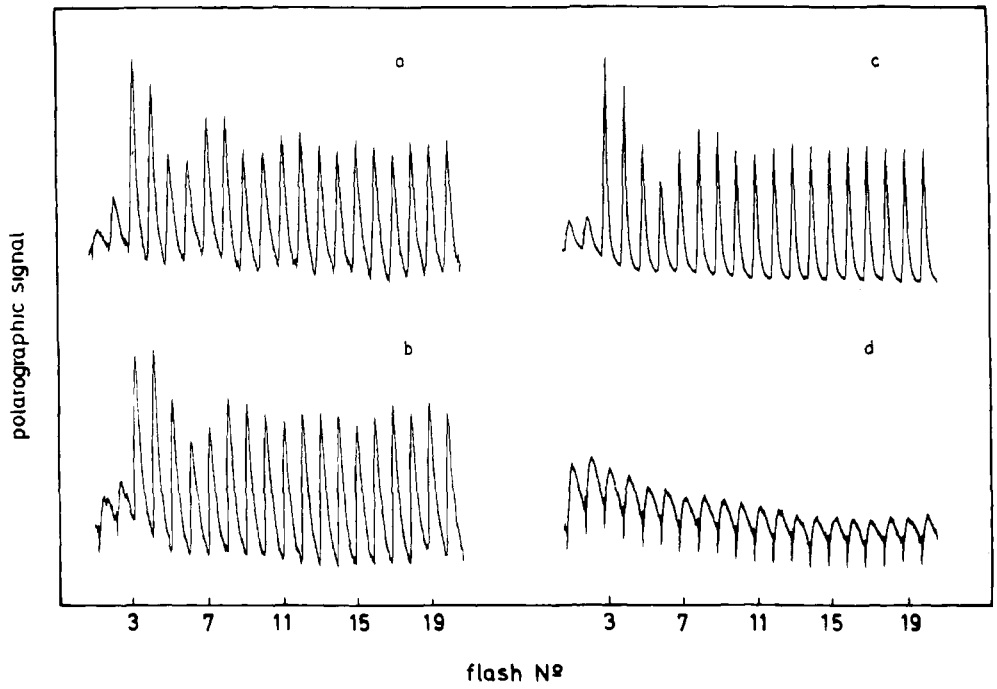

FIGURE 1: Polarographic signals detected by a Joliot-type electrode in cells of WT (traces a and b) and mutant Δ(A373−D380) (traces c and d) that were pre-illuminated for 5 min and subsequently dark-adapted for 5 min (traces a and c) or 24 h (traces b and d). After this dark adaptation, the oxygen yield oscillation pattern was determined as described in Materials and Methods.

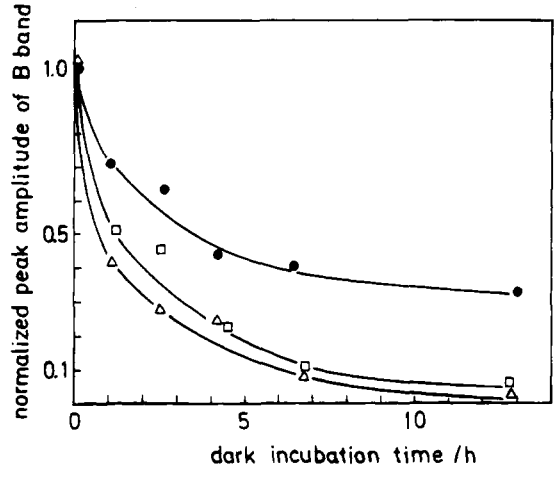

FIGURE 2: Normalized amplitude of the thermoluminescence B-band emission as a function of time between a period of 3 min of pre-illumination of the cells and excitation with a single actinic flash in wild type (●) and mutants Δ(A373−D380) (△) and Δ(R384−V392) (□).

measured in light-activated samples after a short (5 min) dark incubation time. Figure 2 shows the normalized peak height as a function of dark incubation time. The WT exhibits a decline down to a level of about 40%, corresponding with the decrease in the ratio Y_3/Y_6 (vide infra). An almost normal B-band can be observed after two preflashes (data not shown). On the other hand, the amplitudes of the B-band in the mutants Δ(A373−D380) and Δ(R384−V392) completely disappear after sufficient dark incubation.

For a more detailed analysis of the modification of the WOC during dark adaptation, the ratio of the oxygen yield due to the third and sixth flashes, Y_3/Y_6, was measured as a function of the dark incubation time after a 5 min pre-illumination. The Y_3/Y_6 ratio provides a qualitative measure of the WOC dark redox state, because the normalized value Y_3 reaches its maximum if the initial population probability of state S_1 is 1 before illumination with the flash train and, analogously, the normalized Y_6 value is the maximum yield in the sequence at a high population of state S_{-2} [for detailed discussions, see Messinger and Renger (1993)]. It was found that, in WT and all mutants analyzed in this study, the ratio Y_3/Y_6 normalized to the maximum value $(Y_3/Y_6)_{max}$ decreased with progressing dark incubation at room temperature (data not shown).

In general, a change in the oscillation pattern of flash-induced oxygen evolution and in particular the decrease in $(Y_3/Y_6)/(Y_3/Y_6)_{max}$, as well as the decline in the thermoluminescence B-band with progressing dark incubation of WT cells, can be consistently explained by a dark reduction of the WOC below the level of redox state S_1. In order to check this idea, oscillation patterns of the flash-induced oxygen yield were measured at different dark incubation times and evaluated within the framework of the extended Kok model [for a detailed description, see Messinger et al. (1991)]. Figure 3 presents the results obtained by deconvolution of the oscillation pattern based on the conventional approximation of constant probabilities of misses and double hits in all redox transitions of the WOC [for a discussion of dependencies on the redox states of the acceptor and donor sides, see Renger and Hanssum (1988) and Shinkarev and Wraight (1993)]. The numerical fit procedure gives rise to values of $\alpha = 0.15-0.20$ and $\beta = 0.03-0.05$. Interestingly, the parameters α and β appeared to be virtually invariant to the extent of dark incubation. The most prominent feature, however, is the decrease in the S_1 population and a concomitant increase in S_0 to stationary levels. It is important to note that a suitable fit of the oscillation patterns measured at longer dark incubation times requires in addition a population of redox states S_{-1} and, to a minor extent, of S_{-2}. In this analysis, the redox state of the tyrosine residue, Y_D, has not been considered explicitly. Therefore, it is possible that the apparent increase in S_0 population could

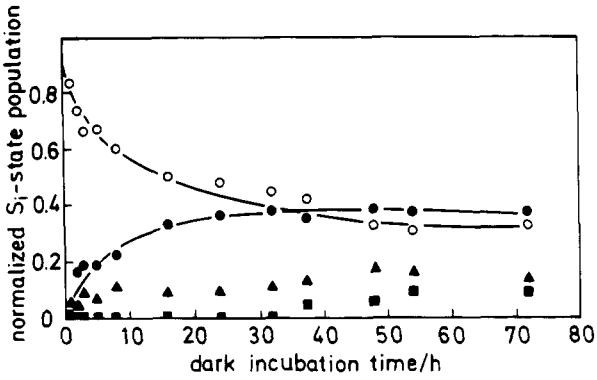

FIGURE 3: Normalized S_i state population $[S_i]$ as a function of dark incubation time between a period of 5 min of pre-illumination and the train of actinic flashes in WT cells. Experimental conditions and calculations were as described in Materials and Methods and in Messinger et al. (1991). Symbols: ○, $[S_1]$; ●, $[S_0]$; ▲, $[S_{-1}]$ and ■, $[S_{-2}]$.

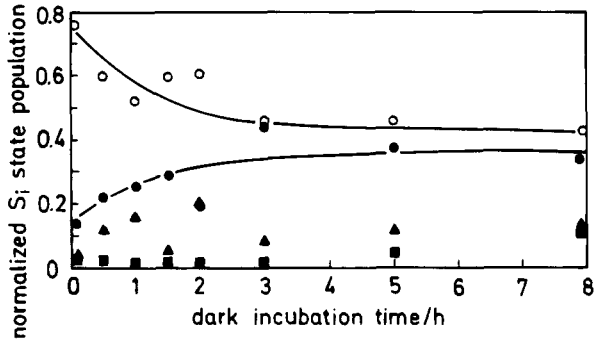

FIGURE 4: Normalized S_i state population $[S_i]$ as a function of dark incubation time between a period of 5 min of pre-illumination and the train of actinic flashes in cells of the mutant Δ(A373−D380). Experimental conditions and calculations were as described in Materials and Methods and in Messinger et al. (1991). Symbols ○, $[S_1]$; ●, $[S_0]$; ▲, $[S_{-1}]$ and ■, $[S_{-2}]$.

be caused to a significant extent by a fast Y_D-induced reduction in S_2 and S_3 [for a recent discussion, see Messinger and Renger, 1994]. However, the appearance of the redox states S_{-1} and S_{-2} indicates that a high population of Y_D is not sufficient to explain the changes in the oscillation pattern during extensive dark incubation of the cells. Regardless of the particular point of possible contributions due to fast S_2 and S_3 decay by Y_D, however, the data obtained with the wild type can be consistently explained by a slow dark reduction of the PSII donor side without the necessity of introducing further assumptions, e.g., a decrease in the total number of functionally competent water-oxidizing complexes.

In marked contrast to this property of the WT, a population of S_0 (S_{-1}, S_{-2}) and/or reduced Y_D alone cannot account for the decline in $(Y_3/Y_6)/(Y_3/Y_6)_{max}$ and in the B-band in mutants Δ(A373−D380) and Δ(R384−V392). At comparatively short dark incubation times of several hours, qualitatively the same changes in the calculated normalized S_i state population are observed as in the WT cells, as is illustrated by the results depicted in Figure 4. However, the further decline in $(Y_3/Y_6)/(Y_3/Y_6)_{max}$ (data not shown) and especially the changes in the signal shape after extensive dark adaptation are indicative of more severe modifications in mutants Δ(A373−D380) (see Figure 1) and Δ(R384−V392) (not shown), leading to a loss of the functional integrity of the WOC. In this case, the polarographic artifact signals arise

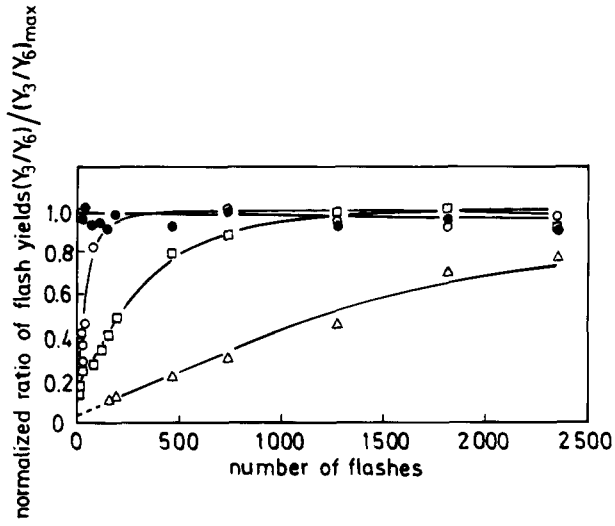

FIGURE 5: Ratio Y_3/Y_6 of the oxygen yields caused by the third (Y_3) and sixth (Y_6) flashes normalized to the maximum value $(Y_3/Y_6)_{max}$, as a function of the number of preillumination flashes given to cells of WT (●) and mutants Δ(A373−D380) (○), Δ(R384−V392) (△) and Δ(D416−F420) (□) after a dark incubation of 48 h. Experimental details of the pre-illumination protocol are described in Materials and Methods.

and prevent any reliable deconvolution of the observed oscillation pattern into S_i state populations. Therefore, the analysis of Figure 4 is restricted to a rather short time domain compared to Figure 3 (in WT the artifact signals are always rather small). It has to be emphasized that the presumed dark inactivation in these mutants does not cause an irreversible suppression of the water-oxidizing capacity, because after sufficient light treatment the oxygen evolution reappears as discovered in a preceding report (Gleiter et al., 1994).

Photoactivation. In order to study the phenomenon of photoactivation in more detail, the effect of excitation with repetitive flashes was analyzed in WT and mutants Δ(A373−D380), Δ(R384−V392) and Δ(D416−F420) by measuring flash-induced oscillation patterns of oxygen yield after a certain number of preflashes, as outlined in Materials and Methods. The normalized ratio $(Y_3/Y_6)/(Y_3/Y_6)_{max}$ was used as qualitative measure for the reconstitution of the WOC, with a normal period four oscillation exhibiting the maximum oxygen yield after the third flash. The results obtained and depicted in Figure 5 show that a rather small number of flashes is sufficient to achieve complete restoration of the normal feature in dark-adapted WT cells. This finding is confirmed by thermoluminescence measurements, revealing almost normal behavior after two preflashes (data not shown). In contrast, more than 2000 flashes are required in order to achieve the optimum oscillation pattern in mutant Δ(R384−V392). The other strains exhibit intermediate behavior [for the sake of clarity, data are not depicted in Figure 5 for mutants Δ(G333−I336), Δ(K347−R352), and Δ(V392−Q394)], with the following order of mutants with respect to the flash numbers N_{PA} necessary for photoactivation: N_{PA}-(Δ(K347−R352)) ≈ N_{PA}(Δ(V392−Q394)) < N_{PA}(Δ(G333−I336)) ≈ N_{PA}(Δ(A373−D380)) < N_{PA} (ΔD416−F420)) ≪ N_{PA} (Δ(R384−V392)). Interestingly, the two mutants Δ(A373−D380) and Δ(R384−V392) are characterized by a very similar time course of the WOC inactivation during dark incubation, but they markedly differ in the N_{PA} values for photoactivation. This observation probably reflects

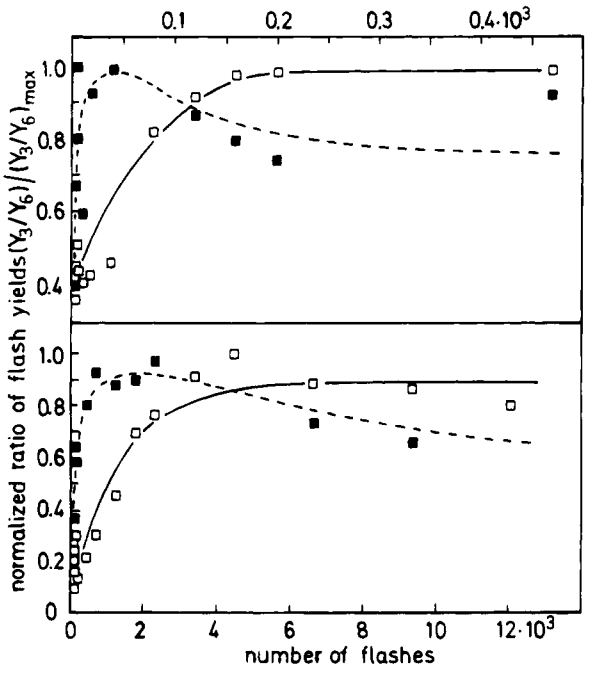

FIGURE 6: Normalized ratio Y_3/Y_6 of the oxygen yield caused by the third (Y_3) and sixth (Y_6) flashes as a function of the number of actinic flashes given to cells of mutants Δ(A373−D380) (top traces) and Δ(R384−V392) (bottom traces) in the absence (□) or presence of 10 mM $CaCl_2$ (■) after dark incubation of 48 h. Experimental details are described in Materials and Methods.

different structural effects on both types of processes, i.e., dark inactivation versus photoactivation (see Discussion).

If the minimum value of Y_3/Y_6 were close to 1, the ratio $(Y_3/Y_6)/(Y_3/Y_6)_{max}$ should be on the order of 0.4−0.5. However, in the case of S_{-1} and S_{-2} formation, the value of Y_3/Y_6 is smaller than 1 [see Messinger and Renger (1994)], and $(Y_3/Y_6)/(Y_3/Y_6)_{max}$ is below 0.4−0.5 as shown in Figure 5. In a previous study, it was shown that, in contrast to the *psbO* deletion mutant completely lacking the PSII-O protein, the *psbB* mutants from Δ(G333−I336) to Δ(D416−F420) do not exhibit a specific elevated Ca^{2+} demand for photoautrophic growth [for a discussion, see Gleiter et al. (1994)]. This indicates that despite different binding affinity in different mutants the presence of the PSII-O protein is sufficient to satisfy the Ca^{2+} requirement for assembling a functionally competent WOC under the illumination conditions of the growth chamber. This conclusion, however, does not necessarily imply that the same is true for the process of photoactivation. Therefore, the effect of Ca^{2+} during the photoactivation process was analyzed in the mutants Δ(A373−D380) and Δ(R384−V392) (the control samples did not exhibit a discernible Ca^{2+} effect; data not shown). The results obtained are depicted in Figure 6. For the sake of easy comparison of the Ca^{2+} effects in mutants Δ(A373−D380) and Δ(R384−V392), the scaling of the abscissa differs by a factor of about 30. The data reveal that in both mutants a significant Ca^{2+}-induced stimulation of photoactivation was observed; i.e., the number of flashes, $N_{1/2}$, required for achieving the half-maximum level of $(Y_3/Y_6)/(Y_3/Y_6)_{max}$ was almost an order of magnitude smaller in the presence of Ca^{2+}, compared with the control in the absence of Ca^{2+}. The stimulatory factor expressed as the ratio $N_{1/2}(+Ca^{2+})/N_{1/2}(-Ca^{2+})$ was similar in both mutants, although the absolute value of $N_{1/2}$ was more than 10-fold in mutant Δ(R384−V392) compared with Δ(A373−D380). These findings

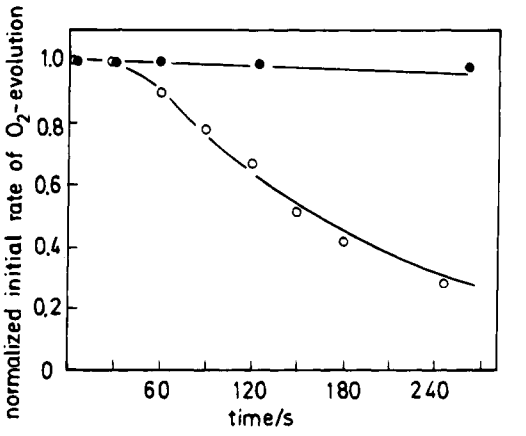

FIGURE 7: Normalized initial rate of light-saturated oxygen evolution as a function of the time of illumination at 5000 μE/m²·s in cells of WT (●) and mutant Δ(A373−D380) (○). The 100% values of the initial rate were 475 and 260 μmol of O_2/mg of Chl·h in WT and mutant Δ(A373−D380), respectively.

clearly show that Ca^{2+} plays an essential role in the photoactivation of the WOC in the mutants.

Photoinhibition. In addition to the very slow dark inactivation of the WOC, some of the mutants also exhibit an enhanced susceptibility to photoinhibition under illumination at a photon flux density of 5000 μE/m²·s. After a short phase (<60 s) of constant activity, the initial rate of mutant Δ(A373−D380) declines to 50% within about 150 s, whereas that of the WT remains virtually unaffected up to 300 s, as shown in Figure 7. This effect strongly depends on the photon flux density. At values of about 500 μE/m²·s the oxygen evolution rate was found to be much more stable in Δ(A373−D380). This explains the sustenance of photoautrophic growth of this mutant for many days in the growth chamber at 60 μE/m²·s. Interestingly, the mutants Δ(G333−I336), Δ(K347−R352), Δ(V392−R394), and Δ(D416−F420) were found to be much less susceptible to photoinhibition at 5000 μE/m²·s (data not shown).

DISCUSSION

The present study is an attempt to analyze the possible role of the Chl *a*-containing integral membrane protein CP47 in establishing a functionally competent water-oxidizing complex (WOC). To address this problem, oscillation patterns of the oxygen yield induced by a train of single-turnover flashes were measured in photoautotrophic mutants that lack 3−8 amino acid residues localized in different regions of the putative large hydrophilic loop E, which is inferred to be exposed to the lumenal side of the thylakoid membrane (Vermaas et al., 1987; Bricker, 1990) and to interact with the manganese-stabilizing extrinsic PSII-O protein (Enami et al., 1987, 1989, 1991; Bricker et al., 1988; Eaton-Rye & Murata, 1989; Frankel & Bricker, 1990; Odom & Bricker, 1992). The results reported here indicate that the different mutants exhibit characteristic changes in the oscillation pattern that are indicative of the stability of the WOC.

Sites of Mutations in Loop E of CP47. Before we discuss these data with respect to dark-induced modifications and processes of photoactivation, it is worth considering the sites of mutation within the framework of fragmentary information that is available on the structure of CP47. Figure 8 shows a schematic picture of the CP47 topology in the thylakoid

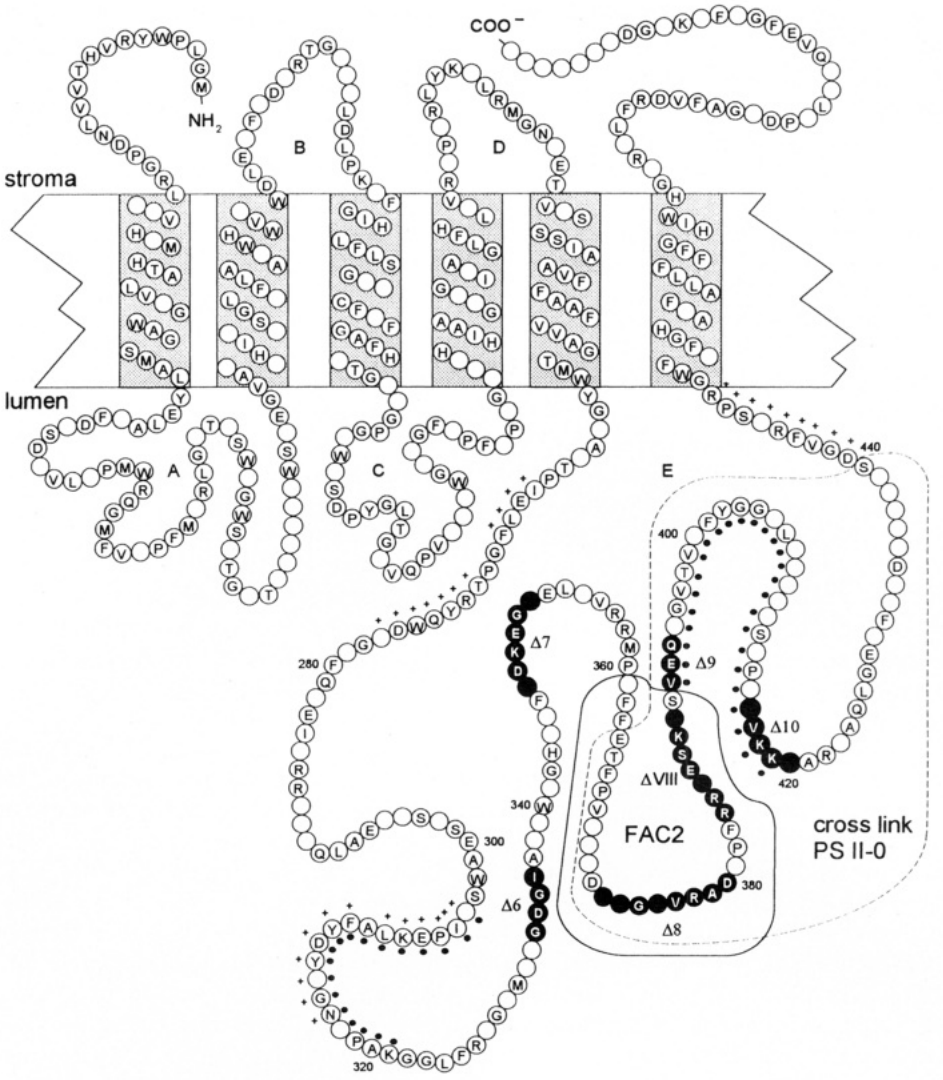

FIGURE 8: Topology of CP47 based on the hydropathy analysis (Vermaas et al., 1987). Only amino acid residues that are conserved between *Synechocystis* sp. PCC 6803 and spinach (*Spinacea oleracea*) are explicitly given. The enclosed areas describe regions of antigenic determinants to the monoclonal antibody FAC 2 (Frankel & Bricker, 1989) (solid line) and the area containing sites of cross-linking with the N-terminus of the PSII-O protein (Odom & Bricker, 1992). Dots indicate regions of NHS-biotinylation in samples depleted of the PSII-O protein (Frankel & Bricker, 1992). The regions indicated by solid residues are domains that can be deleted without loss of autotrophic growth and oxygen evolution, and upon deletion of regions indicated with crosses mutants grow only photoheterotrophically and are not able to assemble a stable PSII complex. Mutants with strongly restricted photoautotrophic growth and drastically reduced PSII content are not shown [for details, see Haag et al. (1993)]. The following abbreviations were used to symbolize the mutants [see also Haag et al. (1993)]: Δ6, Δ(G333−I336); Δ7, Δ(K347−R352); Δ8, Δ(A373−D380); Δ VIII, Δ(R384−V392); Δ9, Δ(R392−Q394); and Δ10, Δ-(D416−F420).

membrane, derived from a hydropathy analysis based on the primary structure obtained by using the sequence of the *psbB* gene encoding CP47 (Vermaas et al., 1987; Bricker, 1990). In a previous report, the locus of the deletion within loop E was shown to be essential for the properties of these mutants (Haag et al., 1993). Most mutants with deletions in loop E fall in one of the following categories: (a) type I has completely lost the capability to grow photoautotrophically and to assemble a stable PSII core complex (symbolized in Figure 8 by crosses (+) next to the amino acid residues that are lacking in the corresponding deletion mutant; for the sake of simplicity, mutants with drastically reduced content and activity of PSII are not shown in Figure 8); (b) type II grows photoautotrophically and exhibits initial oxygen evolution rates of ≥50% of that in the control [see Haag et al. (1993)] (these mutants are symbolized by regions of solid residues with white lettering). Here only type II mutants were analyzed. Interestingly, in these species the amino acid residues are deleted from the same domain(s) (or adjacent regions) of loop E that was (were) previously shown to carry antigenic determinants to the monoclonal antibody FAC2 (Frankel & Bricker, 1989) (area encircled by a full line) or to contain sites of cross-linking with the N-terminus of the PSII-O protein (Odom & Bricker, 1992) (this area is encircled by a dotted line). Furthermore, the above-mentioned regions of loop E are also susceptible to NHS biotinylation after removal of the extrinsic PSII-O protein (Frankel & Bricker, 1992).

The results reported here indicate that the functional manganese cluster within the WOC becomes significantly destabilized in the case of a structural distortion in loop E of CP47 by the deletion of 3−8 amino acid residues from the domain(s) that is (are) inferred to be essential for the binding of the PSII-O protein (Eaton-Rye & Murata, 1989; Frankel & Bricker, 1990; Odom & Bricker, 1992). Two alternative models can be offered to explain this phenom-

enon: (i) loop E directly acts as a stabilizing unit, and weakening of the binding to the PSII-O protein (Gleiter et al., 1994) is a consequence of the modified structure; (ii) loop E has an indirect function in the binding of the extrinsic PSII-O protein that is inferred to stabilize the manganese cluster [for recent reviews on the role of the PSII-O protein, see Debus (1992), and Vermaas et al. (1993)].

The latter idea might be supported by the observation that *psbO* deletion mutants of *Synechocystis* sp. PCC 6803 and *Synechococcus* sp. PCC 7942 exhibit qualitatively the same features of dark inactivation and photoactivation (Engels et al., 1994) as described here for the type II *psbB* mutants. On the other hand, the properties of the *psbO*$^-$ mutants can also be explained by the assumption that binding of the PSII-O protein regulates the structure of loop E, thereby eliciting the stabilization of the functional manganese cluster in the WOC. Alternatively, both structural elements (loop E of CP47 and the PSII-O protein) could directly contribute to the high stability.

A straightforward decision between alternatives i and ii cannot be achieved at our current stage of knowledge. However, some indirect lines of evidence can be gathered from a comparison of type II *psbB* mutants with *psbO*$^-$ mutants from cyanobacteria.

Possible Role of Loop E of CP47 in Relation to Ca^{2+} Effects. It was found that with respect to the Ca^{2+} demand for photoautotrophic growth marked differences exist between the *psbB* mutants described here and the *psbO* deletion mutants completely lacking the PSII-O protein: The former mutants exhibit virtually the same behavior as the WT (Haag et al., 1993), while the maximum growth rate of *psbO*$^-$ mutants requires a markedly higher Ca^{2+} concentration in the assay medium than that of the WT (Burnap & Sherman, 1990; Philbrick et al., 1991; Bockolt et al., 1991; Mayes et al., 1991; Burnap et al., 1992; Vass et al., 1992). On the other hand, a pronounced stimulatory effect of Ca^{2+} was found for the photoactivation of the WOC in thoroughly dark-adapted *psbB* mutants (see Figure 6 of this study). This finding can be explained by the assumption that Ca^{2+} modulates the structure of loop E (vide infra). As a ramification of this idea, Ca^{2+}-induced structural changes in loop E of CP47 could also be responsible for the partial reactivation of oxygen evolution in samples deprived of their PSII-O protein either by genetic engineering (*psbO*$^-$ mutants) or by salt washing [for reviews, see Debus (1992) and Rutherford et al. (1992)].

The above-mentioned results, together with the lack of correlation between the binding strength of the PSII-O protein in different *psbB* mutants [see Gleiter et al. (1994)] and the stability of their WOC to dark inactivation (this study), strengthen the idea that loop E of CP47 is an essential structural unit with its own role in establishing a functionally competent WOC. In this respect, it must be emphasized that the putative loop E has an unusual length of 192 amino acid residues, provided that the topology model of CP47 (see Figure 8) is correct. In this case, loop E has nearly the same size as the psbQ protein of higher plants, which contains 186 amino acids (Jansen et al., 1987). This similarity is another striking feature in favor with the idea that loop E not only connects membrane helices V and VI of CP47 but it probably acts as a specific structural unit in a manner similar to other separate regulatory subunits at the lumenal side of the PSII complex. This implies questions on the possible role of loop E in providing ligands to the coordination sphere of the manganese cluster. However, none of the residues within the deletions discussed here is a likely manganese ligand because recent studies of thermoluminescence, flash-induced changes in the fluorescence quantum yield and oxygen oscillation pattern, and lifetime measurements of S_2 and S_3 did not reveal significant changes in the mutants compared with WT (Gleiter et al., 1994). Therefore, the modifications in loop E due to short deletions of 3−8 amino acids do not cause marked alterations in the redox properties of WOC as would be expected for marked changes in direct manganese ligation by one of the deleted amino acids.

Mechanism of Dark Deactivation and Photoactivation. The evaluation of the oxygen yield oscillation patterns measured at different dark incubation times (Figure 4) shows that a transition to superreduced S_i states (S_{-1}, S_{-2}, S_{-3}?) cannot account for the observed features in the *psbB* mutants where loop E is truncated by 3−8 amino acid residues. This conclusion is fully consistent with the requirement of a large number of flashes (up to a few thousands, depending on the type of the mutant) to restore the normal period four oscillation (see Figure 5). On the basis of these findings, the WOC of the mutants is inferred to undergo a slow (order of hours) dark transition into a functionally incompetent state. The nature of this state is unresolved. However, an irreversible loss of the manganese can be excluded because photoactivation does not require the addition of exogenous manganese. The transition into a nonfunctional WOC is probably a reductive disassembly of the manganese cluster that might comprise the transient formation of superreduced S_i states. This idea is supported by the finding of an increased population probability of S_{-1} and S_{-2} at moderate dark incubation times. In contrast to spinach thylakoids treated with NH_2NH_2 or NH_2OH (Messinger & Renger, 1993), a high population of S_{-1} and S_{-2} was not observed during the process of slow dark inactivation of the WOC in the *psbB* mutants in the absence of exogenous reductants. This could be explained by the assumption that these states are rather unstable in the mutants, i.e., the manganese cluster rapidly degrades in S_{-1} and S_{-2}. In the fully inactivated state, at least part of the manganese is assumed to attain the redox level Mn(II) in a highly distorted structure compared with a functionally competent cluster. This idea is supported by previous findings in spinach PSII membrane fragments deprived of the PSII-O protein by $CaCl_2$ washing (Ono & Inoue, 1983). Suspension of these samples at low Cl^- concentration leads to the formation of Mn(II) that remains bound to the protein in a magnetically uncoupled state (Mavankal et al., 1987). Interestingly, the magnetic coupling can be restored by resuspension at high Cl^- concentration. This effect is ascribed to structural changes induced by these specific ions. A similar structural change due to $CaCl_2$ addition could be responsible for the marked stimulation of photoactivation in the *psbB* mutants observed in this study.

A fully competent WOC can be reestablished by illumination with single-turnover flashes. The number of flashes required to restore the normal period four oscillation pattern of flash-induced oxygen evolution strongly depends on the locus of shortening of loop E by deletion of 3−8 amino acid residues (see Figure 6). The assembly and activation of the manganese cluster in the WOC were shown to be a multistep low quantum yield process that comprises the following

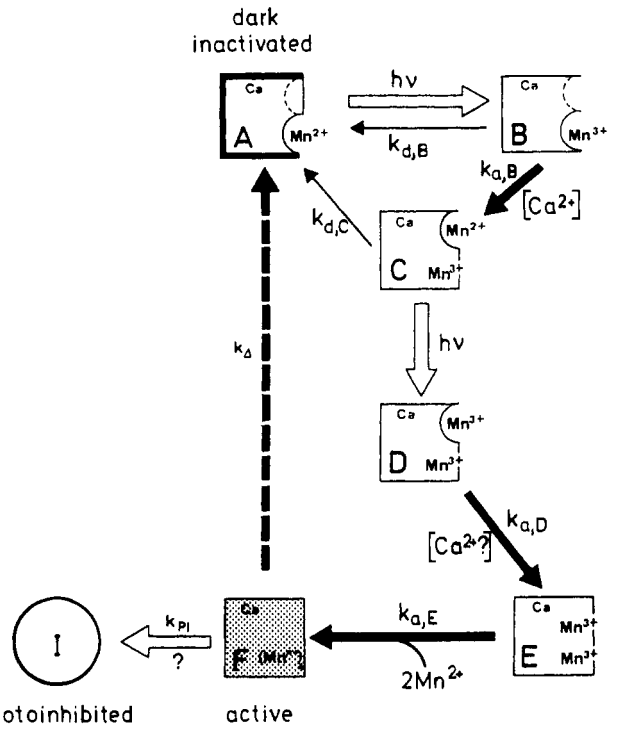

FIGURE 9: Model of dark inactivation and photoactivation of the water-oxidizing complex in cyanobacterial *psbB* mutants. The scheme is based on the model of photoactivation proposed by Tamura and Cheniae (1987). In addition, the process of photoinhibition of oxygen evolution is included and symbolized by an overall rate constant k_{PI}. The rate constants $k_{a,B}$, $k_{a,D}$, and $k_{a,F}$ describe dark reactions in the forward direction of photoactivation symbolized by thick dark arrows; back reactions of intermediary states (B and C) into the dark-inactivated state A are indicated by thin arrows and rate constants $k_{d,B}$ and $k_{d,C}$, respectively, whereas a thick broken arrow and rate constant k_Δ describe the very slow dark transition from a fully competent WOC (state F, dotted area) into the inactive state A. The symbol Ca indicates that the cells contain sufficient Ca^{2+} to sustain photoautotrophic growth, and $[Ca^{2+}]$ symbolizes putative effects of Ca^{2+} on particular dark activation steps coupled with conformational changes. For further details, see the text.

reactions (Tamura & Cheniae, 1987; Ono & Inoue, 1987; Klimov et al., 1990; Miyao & Inoue, 1991; Blubaugh & Cheniae, 1992): (i) photooxidation of a bound Mn^{2+} by Y_Z^{ox}; (ii) formation in the dark of an unstable binuclear $Mn^{2+}-Mn^{3+}$ center by ligation of a second Mn^{2+} ion; (iii) photooxidation of the Mn^{2+} in this center, leading to a stable $Mn^{3+}-Mn^{3+}$ complex; and (iv) insertion of two additional Mn^{2+} ions and subsequent oxidation to the functionally competent tetranuclear manganese cluster. If one assumes that the photoactivation of the WOC in thoroughly dark-incubated *psbB* mutants occurs via an analogous mechanism, the results presented in this study on inactivation, photoinhibition, and photoactivation can be described on the basis of a model for photoactivation proposed by Blubaugh and Cheniae (1992), as outlined in a modified and extended version depicted in Figure 9.

It is proposed that after extensive dark incubation of mutants Δ(A373−D380) and Δ(R384−V392) the WOC attains a state A that is characterized by disassembled manganese with unknown binding sites for the Mn^{2+}. On the basis of the lack of a Ca^{2+} requirement for photoautotrophic growth, it appears very likely that Ca^{2+} is retained in the protein to an extent that is sufficient to ensure the formation of a functionally competent WOC. However, the pronounced effect of Ca^{2+} on the flash-induced photoactivation in both mutants (see Figure 6) indicates that the remaining Ca^{2+} does not satisfy the condition for optimal photoactivation. Illumination of samples in state A leads to the formation of state B by photooxidation of Mn^{2+} and suitable ligation. The subsequent dark transition to state C comprises a structural change that possibly requires Ca^{2+}. A light reaction in state C causes the photooxidation of Mn^{2+} and proper ligation of the Mn^{3+} to establish a stable binuclear $Mn^{3+}-Mn^{3+}$ cluster. The quantum yield of this reaction is assumed to depend on the structure of the protein matrix in state B that is affected by Ca^{2+}. It cannot be excluded that Ca^{2+} also influences the subsequent steps leading via state E to the fully assembled manganese cluster in state F. In the dark, state F slowly degrades to the inactive state A. This transition strongly depends on the structure of loop E that is possibly regulated by interaction with the PSII-O protein.

The process of photoinhibition is symbolized by an overall rate constant k_{PI}. The mechanistic details of this process are unknown, but the rate is modulated by the structure of loop E. In this respect, it must be emphasized that the extent of photoinhibition strongly depends on the functional state of the WOC (Blubaugh et al., 1991; Eckert et al., 1991).

The interplay of photoactivation, photoinhibition, and dark inactivation has an important implication, i.e., the population probability of the different states depends on a given illumination (dark incubation) regime. This phenomenon has to be taken into account for functional studies in cyanobacteria and especially in mutants in order to avoid misinterpretations of the experimental data obtained.

Concluding Remarks. The results of this study have shown that loop E of CP47 plays an essential role in the stability and photoactivation of the WOC. A close interaction with the PSII-O protein is also an important factor, as shown by the recent study of Engels et al. (1994). In addition to that, site-directed mutagenesis of the D1 protein in lumen-exposed regions has shown that this protein is an essential constituent of the WOC and that the PSII-O protein also affects the functional consequences of particular mutations in D1 (Chu et al., 1994a,b). Furthermore, various mutations in the D2 protein cause an enhanced photoinhibition of oxygen evolution (Vermaas et al., 1990). If taken together, the data currently available reveal that different polypeptides participate in establishing a functional competent WOC. In future studies the following remains to be clarified: (i) Which polypeptide(s) provide(s) ligands for the first coordination sphere of the manganese? (ii) How do different polypeptides interact to establish a functionally competent and stable WOC?

REFERENCES

Allakhverdiev, S. I., Karacan, M. S., Somer, G., Karacan, N., Khan, E. M., Rane, S. Y., Padhye, S., Klimov, V. V., & Renger, G. (1994) *Biochemistry 33*, 12210−12214.

Babcock, G. T. (1987) in *New Comprehensive Biochemistry* (Amesz, J., Ed.) Vol. 15, Photosynthesis, pp 125−158, Elsevier, Amsterdam.

Bader, K. P. (1994) *Biochim. Biopyhs. Acta 1188*, 213−219.

Bader, K. P., Thibault, P., & Schmid, G. H. (1983) *Z. Naturforsch. 38c*, 778−792.

Blubaugh, D., & Cheniae, G. M. (1992)in *Research in Photosynthesis* (Murata, N., Ed.) Vol. II, pp 361−364, Kluwer, Dordrecht, The Netherlands.

Bockholt, R., Masepohl, B., & Pistorius, E. K. (1991) *FEBS Lett. 294*, 59−63.

Bricker, T. M. (1990) *Photosynth. Res. 24*, 1−13.

Bricker, T. M., & Frankel, L. K. (1987) *Arch. Biochem. Biophys. 256*, 295−301.
Bricker, T. M., Odom, R., & Queirolo, C. B. (1988) *FEBS Lett. 231*, 111−117.
Burnap, R. L., Shen, J.-R., Jursinic, P. A., Inoue, Y., & Sherman, L. A. (1992) *Biochemistry 31*, 7404−7410.
Cheniae, G. M., & Martin, I. F. (1970) *Biochim. Biophys. Acta 895*, 259−274.
Chu, H. A., Nguyen, A. P., & Debus, R. J. (1994a) *Biochemistry 33*, 6137−6149.
Chu, H. A., Nguyen, A. P., & Debus, R. J. (1994b) *Biochemistry 33*, 6150−6157.
Debus, R. J. (1992) *Biochim. Biophys. Acta 1102*, 269−353.
Eaton-Rye, J. J., & Murata, N. (1989) *Biochim. Biophys. Acta 997*, 219−226.
Eaton-Rye, J. J., & Vermaas, W. F. J. (1991) *Plant Mol. Biol. 17*, 1165−1177.
Enami, I., Satoh, K., & Katoh, S. (1987) *FEBS Lett. 226*, 161−165.
Enami, I., Miyaoko, T., Mochizuki, Y., Shen, J.-R., Satoh, K., & Katoh, S. (1989) *Biochim. Biophys. Acta 973*, 35−40.
Enami, I., Kaneko, M., Kitamura, N., Koike, H., Sonoike, K., Inoue, Y., & Katoh, S. (1991) *Biochim. Biophys. Acta 1060*, 224−232.
Engels, D. H., Lott, A., Schmid, H. G., & Pistorius, E. K. (1994) *Photosynth. Res. 42*, 227−244.
Frankel, L. K., & Bricker, T. M. (1989) *FEBS Lett. 257*, 279−282.
Frankel, L. K., & Bricker, T. M. (1990) in *Current Research in Photosynthesis* (Baltscheffsky, M., Ed.) Vol. I, pp 639−642, Kluwer Academic Publishers, Dordrecht, The Netherlands.
Frankel, L. K., & Bricker, T. M. (1992) *Biochemistry 31*, 11059−11064.
Gleiter, H. M., Haag, E., Shen, J.-R., Eaton-Rye, J. J., Inoue, Y., Vermaas, W. F. J., & Renger, G. (1994) *Biochemistry 33*, 12063−12071.
Haag, E. (1993) Ph.D. Thesis, Technical Unviversity Berlin.
Haag, E., Eaton-Rye, J. J., Renger, G., & Vermaas, W. F. J. (1993) *Biochemistry 32*, 4444−4454.
Ikeuchi, M. (1992) *Bot. Mag. Tokyo 105*, 327−373.
Jansen, T., Rother, C., Steppuhn, J., Reinke, H., Beyreuther, K., Jansson, C., Andersson, B., & Herrmann, R. G. (1987) *FEBS Lett. 216*, 234−240.
Joliot, P. (1972) *Methods Enzymol. 24*, 123−134.
Klein, M. P., Sauer, K., & Yachandra, V. K. (1993) *Photosynth. Res. 38*, 265−277.
Klimov, V. V., Ananyev, G., Allakhverdiev, S. I., Zharmukhamedov, S. K., Mulay, M., Hedge, U., & Padhye, S. (1990) in *Current Research in Photosynthesis* (Baltscheffsky, M., Ed.) Vol. I, pp 247−254, Kluwer, Dordrecht, The Netherlands.
Kok, B., Forbush, B., & McGloin, M. (1970) *Photochem. Photobiol. 11*, 457−475.
Kusunoki, M., Ono, T., Noguchi, T., Inoue, Y. & Oyanagi, H. (1993) *Photosynth. Res. 38*, 331−340.
Mavankal, G., McCain, D. C., & Bricker, T. M. (1987) in *Progress in Photosynthesis Research* (Biggins, J., Ed.) Vol. I, pp 661−664, M. Nijhoff, Dordrecht, The Netherlands.
Mayes, S. R., Cook, K. M., Self, S. J., Zhang, Z., & Barber, J. (1991) *Biochim. Biophys. Acta 1060*, 1−12.
Messinger, J., & Renger, G. (1990) *FEBS Lett. 277*, 141−146.
Messinger, J., & Renger, G. (1993) *Biochemistry 32*, 9379−9386.
Messinger, J., & Renger, G. (1994) *Biochemistry 33*, 10896−10905.
Messinger, J., Wacker, U., & Renger, G. (1991) *Biochemistry 30*, 7852−7862.
Miyao, M., & Inoue, Y. (1991) *Biochemistry 30*, 5379−5387.
Mukerji, J., Andrews, J. C., DeRose, V. J., Latimer, M. J., Yachandra, V. K., Sauer, K., & Klein, M. P. (1994) *Biochemistry 33*, 9712−9721.
Odom, W. R., & Bricker, T. M. (1992) *Biochemistry 31*, 5616−5620.
Ono, T.-A., & Inoue, Y. (1983) *FEBS Lett. 164*, 225−260.
Ono, T.-A., & Inoue, Y. (1987) *Plant Cell Physiol. 28*, 1293−1299.
Philbrick, J. B., Diner, B. A., & Zilinskas, B. A. (1991) *J. Biol. Chem. 266*, 13370−13376.
Radmer, R., & Cheniae, G. M. (1977) in *Primary Processes of Photosynthesis* (Barber, J., Ed.) Vol. 2, pp 303−348, Elsevier, Amsterdam.
Renger, G. (1987a) *Angew. Chem., Int. Ed. Engl. 26*, 643−660.
Renger, G. (1987b) *Photosynthetica 21*, 203−224.
Renger, G. (1993) *Photosynth. Res. 38*, 229−247.
Renger, G., & Hanssum, B. (1988) *Photosynth. Res. 16*, 243−259.
Rippka, R., Deruelles, J., Waterbury, J. B., Herdman, M., & Stanier, R. Y. (1979) *J. Gen. Microbiol. 111*, 1−61.
Rutherford, A. W., Crofts, A. R., & Inoue, Y. (1982) *Biochim. Biophys. Acta 682*, 457−465.
Rutherford, A. W., Renger, G., Koike, H., & Inoue, Y. (1984) *Biochim. Biophys. Acta 767*, 548−556.
Rutherford, A. W., Zimmermann, J. L., & Boussac, A. (1992) in *The Photosystems: Structure, Function and Molecular Biology* (Barber, J., Ed.) pp 179−229, Elsevier, Amsterdam.
Seibert, M., & Lavorel, J. (1983) *Biochim. Biophys. Acta 723*, 160−168.
Shinkarev, V. P., & Wraight, C. A. (1993) *Photosynth. Res. 38*, 315−321.
Tamura, N., & Cheniae, G. M. (1987) *Biochim. Biophys. Acta 890*, 179−194.
Tamura, N., Kamachi, H., Hokari, N., Matsumoto, H., & Inoue, H. (1991) *Biochim. Biophys. Acta 1060*, 51−58.
Vass, I., & Inoue, Y. (1992) in *Topics in Photosynthesis, The Photosystems: Structure, Function and Molecular Biology* (Barber, J., Ed.) pp 259−294, Elsevier, Amsterdam.
Vass, I., Cook, K. M., Deák, Z., Mayes, S. R., & Barber, J. (1992) *Biochim. Biophys. Acta 1102*, 195−201.
Vermaas, W. F. J., Williams, J. G. K., & Arntzen, C. J. (1987) *Plant Mol. Biol. 8*, 317−326.
Vermaas, W. F. J., Charité, J., & Shen, G. (1990) *Biochemistry 29*, 5325−5332.
Vermaas, W. F. J., Styring, S., Schröder, W. P., & Andersson, B. (1993) *Photosynth. Res. 38*, 249−264.
Yachandra, V. K., de Rose, V. J., Latimer, M. J., Mukerji, I., Sauer, K., & Klein, M. P. (1993) *Science 260*, 675−679.

BI942919Z